This paper was originally published as an *ASHRAE Transactions paper* and may be cited as:

Ndiaye, D. and M. Bernier. 2014. One and Two Time Constant Models to Predict the Capacity of Geothermal Heat Pumps in Cycling Conditions. ASHRAE Transactions, 120(2): 320-333.

One- and Two-Time-Constant Models to Predict the Capacity of Geothermal Heat Pumps in Cycling Conditions

Demba Ndiaye, PhD, PE
Member ASHRAE

Michel Bernier, PhD, PE
Member ASHRAE

ABSTRACT

Generalized one- and two-time-constant models used to capture the evolution of the capacity of geothermal heat pumps at compressor start-up are presented. A one-time-constant model for the capacity decay at compressor shutdown is also presented. The determination of these time constants is important as longer time constants lead to more degradation of the heat pump performance in cycling conditions. Various reference time constants are obtained from a detailed and experimentally validated dynamic model of a geothermal heat pump in a range of operating conditions in heating or cooling mode. These dynamic empirical models are efficient and are more appropriate to whole-building energy simulation than corresponding deterministic models. It is shown that, contrary to the impression that may come from the literature, time constants change according to operating conditions. In particular, if the runtime decreases, the time constants tend to increase in the heating mode and to decrease in the cooling mode. They increase with the inlet water temperature (IWT) and decrease if the pressures are allowed to equalize at compressor shutdown. Finally, the time constants tend to increase when the fan is continuously operating. A time-constant-based heat pump model is derived and implemented in the dynamic energy simulation software TRNSYS.

INTRODUCTION

Geothermal heat pumps allow for a notable reduction in building energy consumption. Since ground temperature remains almost constant yearlong, geothermal heat pumps can operate all the time providing heat or cold according to demand, with coefficients of performance in the order of three to five. Better modeling of such heat pumps leads to energy simulations that are closer to reality. One area that deserves attention is the noticeable degradation of heat pump performance in cycling conditions due to the gradual evolution of the capacity at start-up. Depending on operating conditions, the heat pump can lose up to 20% in capacity (Katipamula and O'Neal 1991). This phenomenon is due to thermal masses and refrigerant migrations when heat pumps are switched off and the resulting gradual evolution of the capacity towards a steady-state value at compressor start-up. It is thus important to accurately capture this evolution in the simulation model and this is the main subject of the present investigation.

Two main approaches are used to evaluate the evolution of the capacity at start-up: dynamic empirical models, and dynamic deterministic models. Empirical models are generally based on a time constant or on other correlations. Deterministic models are based on the governing equations describing the physics of the phenomenon being studied. Deterministic models of heat pumps are relatively complex and time consuming, and are not appropriate for whole-building energy analysis. Thus, empirical models are preferred in this situation.

Regarding dynamic empirical models, the evolution of the capacity $\dot{Q}$ at compressor start-up has been seen as a first order function giving:

$$\dot{Q} = \dot{Q}_{SS}(1 - e^{-t/\tau}) \quad (1)$$

where $\dot{Q}_{SS}$ is the value of the capacity at steady-state conditions, t is time, and τ is the time constant of the system. Various authors have used this model; for example: Murphy and Goldschmidt (1979), Goldschmidt et al. (1980), Katipamula and O'Neal (1991), and O'Neal and Katipamula (1991). In the format of Equation 1, Mulroy and Didion (1985) and Votsis et

Demba Ndiaye is a senior energy analyst/mechanical engineer at Setty & Associates, Fairfax, VA and **Michel Bernier** is a professor in the Département de Génie Mécanique, École Polytechnique de Montréal, Montréal, QC, Canada.

al. (1992) proposed a two-time-constant (t_1 and t_2) model of the form:

$$\dot{Q} = \dot{Q}_{SS}\left(1 - Ae^{-t/\tau_2}\right)\left(1 + Be^{-t/\tau_1}\right) \quad (2)$$

At compressor shutdown, if the fan is running continuously, there is a residual capacity that can be modeled using an extinction function (Mulroy and Didion, 1985):

$$\dot{Q} = A\dot{Q}_{SS}e^{-t/\tau} \quad (3)$$

where A is a regression parameter, and τ is the shutdown time constant.

It is not clear from the scarce literature on the subject whether the time constant of a system is a constant value or varies depending on the operating conditions. This paper addresses these questions and proposes values of the time constants under different operating conditions using a detailed and experimentally validated dynamic model of a geothermal heat pump.

BACKGROUND: THE HEAT PUMP MODEL

The modeled water-to-air heat pump has the following configuration: (i) refrigerant-to-water double tube heat exchanger with inner convoluted tube and the refrigerant flowing in the annulus, (ii) refrigerant-to-air copper fin and aluminium tube heat exchanger, (iii) hermetic reciprocating compressor, (iv) thermostatic expansion valve, (v) reversing valve, and (vii) R-22 as the refrigerant (see Figure 1).

To model the refrigerant-to-air heat exchanger, a distributed approach was used. The model has been described elsewhere (see Ndiaye and Bernier 2010b) and will only be briefly described here. For the flow of refrigerant in the tubes, the transient forms of the mass, momentum, and energy conservation

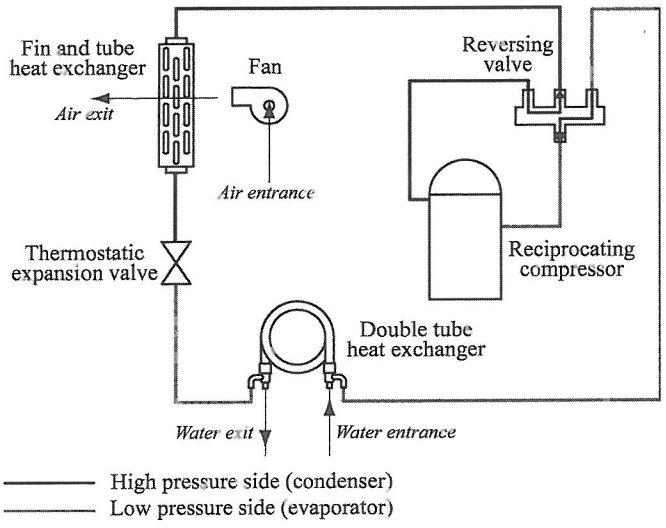

Figure 1 *Schematic representation of the modeled heat pump (shown in heating mode).*

equations were derived for both the single-phase and the two-phase flows. The secondary fluid (air) and the tube walls were modeled with the energy conservation equations. All the governing equations were solved numerically using the finite volume method of Patankar (1980). The two most common configurations for the tubes (rectangular and staggered) were considered. The circuits of the heat exchanger were divided into wall elements. An indexation process that keeps track of the wall elements and the circuits they belong to was also proposed. The modeling of the refrigerant-to-water heat exchanger follows the same principle.

The compressor is certainly the most complex component of the heat pump. The objective of the modeling was to determine the suction and discharge flow rates, the thermodynamic state of the refrigerant at the discharge side based on knowledge of the suction, and discharge pressures and the thermodynamic state of the refrigerant at the suction side. In the modelling of the compressor, the shell was treated as a single lumped element and the discharged refrigerant mass flow rate was determined using a thermodynamic analysis of the compression-expansion process (see Ndiaye and Bernier 2010a).

The thermostatic expansion valve (TXV) can be equipped with a bleed port: a special orifice that allows for the equalization of the pressures at compressor shutdown. As such, and due to the obviously different characteristics of the flow through the main valve and through the relatively small passage of the bleed port, the model of the TXV was separated in two parts. The overall objective of the modeling was to determine the refrigerant flow rate through the TXV independently of the operation state of the heat pump using inputs such as the pressures at the inlet and outlet of the valve and the thermodynamic state of the refrigerant at the inlet of the valve. The model of the flow through the main valve consisted of modeling the dynamic evolution of the state of the refrigerant contained in the bulb and adding a semiempirical model of the refrigerant flow based on an analysis of the dynamics of the valve itself. The flow through the bleed port was modelled using a separated flow model to fully address the four possible flow conditions: (1) inlet liquid, outlet liquid; (2) inlet liquid, outlet two-phase; (3) inlet two-phase, outlet two-phase; and (4) inlet vapour, outlet vapour (see Ndiaye and Bernier 2009).

Additionally, the effects of the reversing valve and of the plenum enclosing the fan were modelled. The model of the heat pump fully accounted for both the on and off operations of the compressor and of the fan.

The global model is the combination of the individual models of the components of the heat pump: the two heat exchangers, the compressor, the expansion valve, the reversing valve, and the fan. A tube is placed at the entrance and exit of each heat exchanger. The bulb of the expansion valve is placed on the tube at the exit of the evaporator.

A commercial heat pump unit with a 3 ton (≈10.6 kW) nominal capacity was used to experimentally validate the global numerical model. The heat pump was instrumented

Table 1. Cases Studied for the Experimental Validation of the Heat Pump Model

Code	Mode	With or Without Bleed Port	Fan Operation at Compressor Shutdown
HTSBFR	Heating	Without	Running
HTSBFS	Heating	Without	Stopped
HTABFR	Heating	With	Running
HTABFS	Heating	With	Stopped
CLSBFR	Cooling	Without	Running
CLSBFS	Cooling	Without	Stopped
CLABFR	Cooling	With	Running
CLABFS	Cooling	With	Stopped

with various devices allowing the measurements of: the temperatures and pressures of the refrigerant at the inlet and outlet of the four major components of the heat pump (the two heat exchangers, the compressor and the expansion valve), the amount of power used by the compressor and the fan, the flow rates of the air and of the water, the inlet and outlet temperatures of the air and of the water, and the inlet and outlet humidity ratios of the air. To reproduce various conditions of operation of the heat pump, eight validation cases were considered while setting cycle duration to 20 min (10 in the on-cycle, 10 in the off-cycle). The eight cases, which will be referred to in the next sections of this paper, correspond to the following combinations: (i) heating (HT) or cooling (CL) mode, (ii) with bleed port (AB) or without bleed port (SB) in the expansion valve, and (iii) fan running (FR) or stopped (FS) at compressor shutdown. The coding for these eight cases is shown in Table 1.

The experiments took place in an environmental chamber to control the air conditions. The experimental data were validated using the principle of energy conservation applied to the steady-state parts of the data. First, it was confirmed that in each heat exchanger, in both heating and cooling modes, the energy lost or gained by the refrigerant was equal to the energy gained or lost by the secondary fluid (air or water). Then, it was confirmed that the energy lost by the refrigerant at the condenser is the sum of the energy it received at the evaporator and the energy it gained at the compressor.

The results of the validation exercise of the heat pump model were satisfactory. As an illustration, Figure 2 presents a comparison between the model predictions and the measured outlet air temperature for the HTSBFR case (heating mode, without bleed port, with fan running continuously). In this figure, Ten is the inlet air temperature and Tex is the outlet air temperature. It can be seen that the simulated outlet air temperature falls within the uncertainty bands of the experimental results. More information on the heat pump model is given in Ndiaye and Bernier (2012a). This model will now be used to derive time constants.

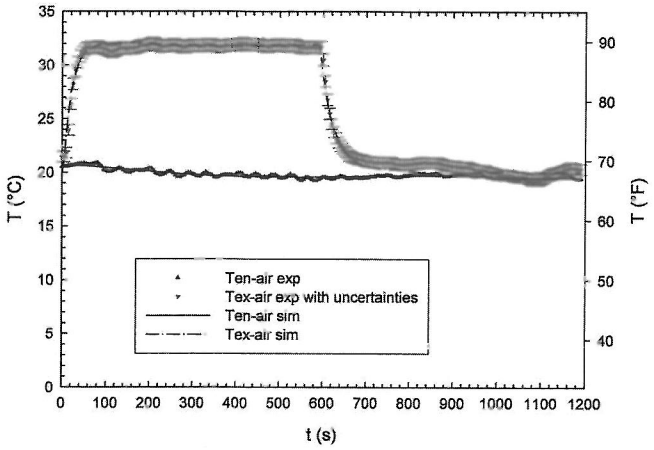

Figure 2 *Comparison between the model and experiments: variation of the outlet air temperature.*

TIME CONSTANT MODELS ASSESSMENT

START-UP

Various time-constant models have been introduced above in Equations 1 and 2. In Equation 2 τ_1 and τ_2 are called "time constants." However, they are not really time constants per the usual meaning of this term but rather simple regression coefficients much like A and B in the same equation. However, for clarity and for comparison purposes, they will be referred to as "time constants" in this text. Consequently, the model in Equation 2 is called a "two-time-constant model."

It can be remarked that the one-time-constant model is a specific case of the two-time-constant model with $B = 0$. It can also be noted that the value of the capacity at start-up ($t = 0$) is:

$$\dot{Q}_0 = \dot{Q}_{SS}(1 - A)(1 + B) \quad (4)$$

Consequently, if the initial value of the capacity is null, as in the cases studied in this paper, $A = 1$. It was also noted from our validation exercise of the heat pump model (results are

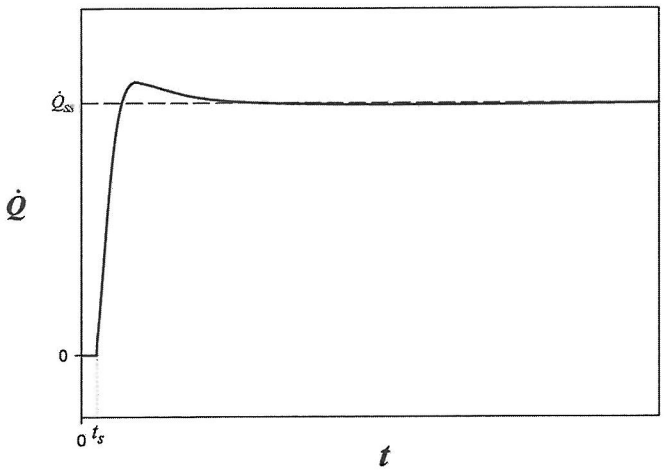

Figure 3 *General format of the variation of the capacity at compressor start-up.*

presented in Figure 4) that the capacity does not always begin rising immediately after the start of the compressor. This is due to the thermal inertia in the air plenum and to a compressor delay of about 15 to 20 s after start-up in cases where the fan is stopped in the off-cycle. Accounting for these two observations, the model becomes:

$$\begin{cases} \dot{Q} = 0 \quad t < t_s \\ \dot{Q} = \dot{Q}_{SS}\left[1 - e^{-(t-t_s)/\tau_1}\right]\left[1 + Be^{-(t-t_s)/\tau_2}\right] \quad \text{for } t \geq s \end{cases} \tag{5}$$

with $t = 0$ at compressor start-up, and t_s is the time required for the capacity to begin to increase (Figure 3). Setting $B = 0$ in Equation 5 leads to the one-time-constant model.

The application of the one- and two-time-constant models to the six base cases (HTSBFR, HTSBFS, HTABFR, HTABFS, CLSBFR, and CLSBFS) allows to assess their performance as shown in Figure 4. The real capacities come from the simulations with the heat pump model.

This figure shows, as evidenced by the R^2 of the regressions, that the two-time-constant model is the most appropriate to represent the evolution of the capacity at compressor start-up. However, the one-time-constant model is simpler and is more prone to generalizations, and thus to comparisons.

Shutdown

The following one-time-constant extinction function allows modelling of the residual capacity at compressor shudown:

$$\dot{Q} = (D\dot{Q}_{SS})e^{-t/\tau_3} + \dot{Q}_R \tag{6}$$

where $t = 0$ at the exact time when the compressor shuts down, D and $\dot{Q}_R$ are regression parameters and τ_3 is the time constant. The presence of D allows to account for the cases where the compressor stops before the full capacity $\dot{Q}_{SS}$ is reached. The parameter $\dot{Q}_R$ allows accounting for the power used by the fan when it is in a continuous operation mode.

Results given by Equation 6 are compared to the heat pump model in Figure 5 where it is shown that the evolution of the capacity at compressor shutdown is well modeled. The dip seen at around $t = 300$ s in Figure 5 is due to a leak in the reversing valve (see Ndiaye 2007). In cases where the fan is off at compressor shutdown (HTSBFS, HTABFS, and CLSBFS), there is also a residual capacity up to about 100 s due mainly to fan delay and inertia.

RESULTS AND DISCUSSIONS

The objective of this section is to obtain the time constants for combinations of the most often encountered operating conditions and see how they vary with operating conditions. The water flow rate is set to 9 gpm (0.568 kg/s) and the airflow rate to 1200 cfm (0.566 m^3/s). Inlet air temperature and humidity ratio are set based on the standard CAN/CSA-C13256-1-01 "Water-Source Heat Pumps – Testing and Rating for Performance" (CAN/CSA 2001): 20°C (68°F) and 0.0086 kg_{water}/kg_{dryair} (0.0086 lb_{water}/lb_{dryair}) respectively in heating mode, and 27°C (80.6°F) and 0.01045 kg_{water}/kg_{dryair} (0.01045 lb_{water}/lb_{dryair}) respectively in cooling mode. The following combinations are studied:

- Mode: heating/cooling (two modalities: HT/CL)
- Bleed port: with/without for heating mode, with for cooling mode (AB/SB)
- Fan operation at compressor shutdown: on/off (two modalities: FR/FS)
- Inlet water temperature (IWT): 5°C (41°F) (code A)/ 15°C (59°F) (code B) in heating mode; 10°C (50°F) (code A)/20°C (68°F) (code B) in cooling mode (two modalities)

The cycle durations given in Table 2 are considered.

The total number of cases studied is 84, i.e., 14 subcases for each of the 6 base cases (HTSBFR, HTSBFS, HTABFS, HTABFR, CLSBFR, and CLSBFS). The subcases of HTSBFR are listed in Table 3 as an example of the coding used. For each subcase, the coding is made of the name of the base case, the code for the IWT (*A* or *B*), the runtime (min), and the off-cycle time (min), in this order. The heat pump that served to validate the model is used.

Tables 4 to 9 present the regression parameters for each of the 84 studied cases. Exponential growth and exponential decay types regression models are used. In the specific case of the cooling mode, time constants are needed for the sensible capacity as well as for the total capacity. Thus, the evolution of the latent capacity, which is the difference between the total capacity and the sensible capacity, may also be known.

For explanations on heat pump behavior when submitted to various operating conditions, refer to Ndiaye and Bernier

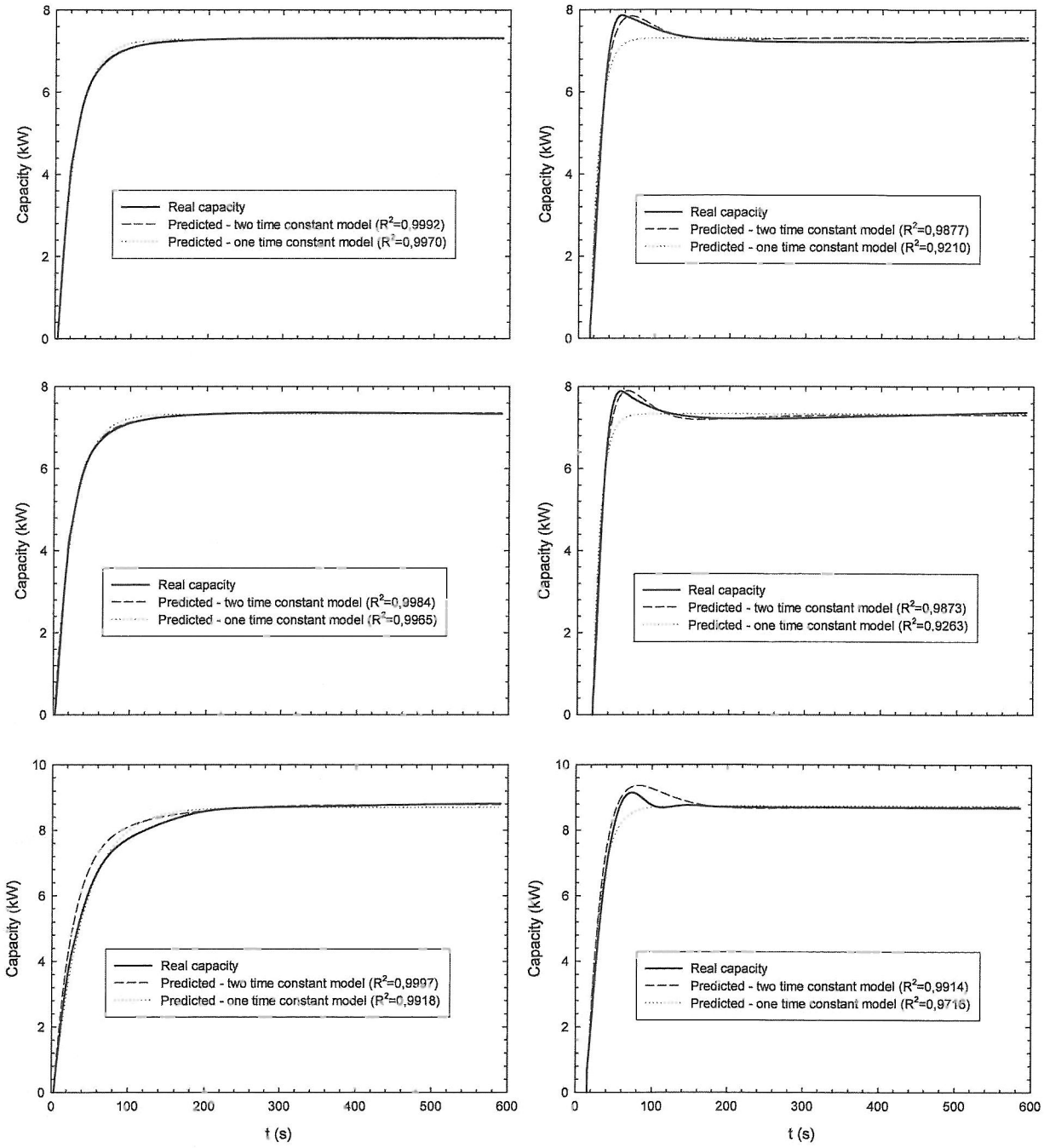

Figure 4 *Modeling the variation of the capacity at compressor start-up.*

(2012b). Here, the focus is on the impact of this behavior on the start-up and shutdown time constants.

Start-up Time Constant(s)

The one-time-constant model is the most often used in modeling the start-up capacity evolution. In consulting the literature, the major impression is that the time constant τ has a constant value for a given machine. However, it may be seen from Tables 4 to 9 that τ varies according to the operating conditions. In the cases presented, the time constant varies from 0.1 s (meaning in that case that the full capacity is reached almost immediately after start-up) to 27.1 s. The time constant at start-up is the time it takes after the capacity begins to increase (i.e., from the time t_s) for it to reach 63.2% of its full-value $\dot{Q}_{SS}$ (steady-state value at the given operating conditions). As the first-order response is an increasing function, if the time constant is higher, then it takes more time for the capacity to get close to its full value.

It is interesting to see how the time constant varies depending on the operating conditions of the heat pump. Using the one-time-constant model, it can be seen that τ varies depending on: (1) runtime; (2) off-cycle time; (3) IWT; (4) operating mode of the fan at compressor shutdown; and (5) presence or not of a bleed port.

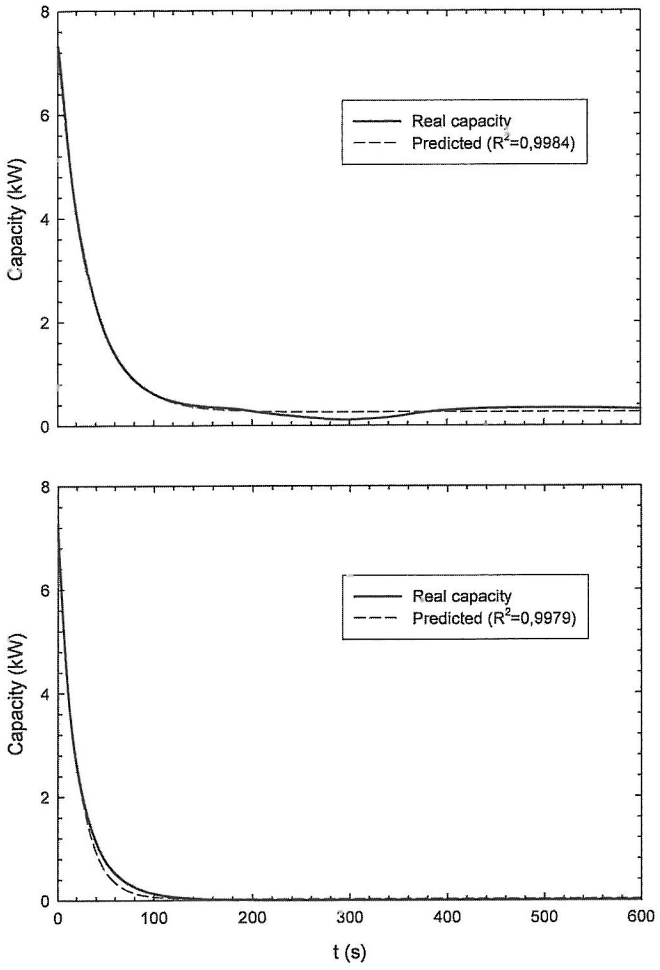

Figure 5 *Modeling the variation of the capacity at compressor shutdown.*

Observing Tables 4 and 5 (Heating mode/Without bleed port cases), the value of τ_1 (average: 23.9 s) at 5°C (41°F) IWT (IWT) and 5 min runtime is slightly inferior to τ_1 (average: 24.4 s) at 15°C (59°F) IWT and the same runtime, which indicates that there is less performance degradation at lower IWT (for a 5 min runtime). As can be seen in the cases of a 10 min runtime/5 min off-cycle time, shorter off-cycle time leads to more performance degradation at start-up (however, that does not happen for the cases with bleed port). With off-cycle times sufficiently long (10 min or more), τ_1 becomes independent of the off-cycle time. Also, with a 10 min runtime, τ_1 at a 5°C (41°F) IWT is inferior to τ_1 at 15°C (59°F) IWT, indicating that τ_1 increases with the IWT.

A similar analysis of the remaining results in Tables 4 to 9 leads to the following conclusions.

Variation of the time constant with respect to runtime. In heating mode, for the cases without bleed port (subcases HTSBFR and HTSBFS) the time constant decreases when the runtime increases.

In the cooling mode, it is noted that the time constant increases with the runtime, except for the case where (1) the fan is not in continuous mode and (2) IWT is 20°C (68°F).

Variation of the time constant with respect to off-cycle time. In the heating mode, when the off-cycle time increases, the time constant increases if the runtime is 5 min, but decreases if the runtime is 10 min.

In the cooling mode, the influence of the off-cycle time on the time constant is rather negligible.

Variation of the time constant with respect to IWT. In the heating mode, as well as in the cooling mode, the time constant increases with the IWT.

Variation of the time constant with respect to fan mode at compressor shutdown. In the heating mode, as well as in the cooling mode, the time constant decreases if the fan is off at compressor shutdown (subcases HTSBFS, HTABFS, and CLSBFS).

Variation of the time constant with respect to the presence or not of a bleed port. The time constant decreases when a bleed port is present compared to when there is none, except if the runtime and off-cycle time are both superior to 5 min.

Table 2. Runtimes and Off-Cycle Times Combinations Studied

Runtime (Off-Cycle Time), min.	Cycle Duration, min	Cycling Rate, Number of Cycles Per Hour	Percent On-time, %
5 (10)	15	4	33
5 (15)	20	3	25
5 (20)	25	2.4	20
10 (5)	15	4	67
10 (10)	20	3	50
10 (15)	25	2.4	40
10 (20)	30	2	33

Table 3. Subcases of Case HTSBFR Studied

Code	IWT, °C (°F)	Runtime, min	Off-Cycle Time, min
HTSBFR-A-5-10	5 (41)	5	10
HTSBFR-A-5-15	5 (41)	5	15
HTSBFR-A-5-20	5 (41)	5	20
HTSBFR-A-10-5	5 (41)	10	5
HTSBFR-A-10-10	5 (41)	10	10
HTSBFR-A-10-15	5 (41)	10	15
HTSBFR-A-10-20	5 (41)	10	20
HTSBFR-B-5-10	150 (59)	5	10
HTSBFR-B-5-15	15 (59)	5	15
HTSBFR-B-5-20	15 (59)	5	20
HTSBFR-B-10-5	15 (59)	10	5
HTSBFR-B-10-10	15 (59)	10	10
HTSBFR-B-10-15	15 (59)	10	15
HTSBFR-B-10-20	15 (59)	10	20

Table 4. Time Constants at Start-up and at Shutdown for the Subcases of Case HTSBFR

Code	Start-up Two-Time-Constant Model				Start-up One-Time-Constant Model		Shutdown	
	t_s, s	B	τ_1, s	τ_2, s	t_s, s	τ_1 s	τ_3, s	$\dot{Q}_R$, kW (kBtu/h)
HTSBFR-A-5-10	0.0	1.52	60.6	49.5	0.0	23.5	27.4	0.34 (1.16)
HTSBFR-A-5-15	0.0	1.50	61.3	50.2	0.0	24.0	27.4	0.34 (1.16)
HTSBFR-A-5-20	0.0	1.60	64.9	51.5	0.0	24.2	27.4	0.34 (1.16)
HTSBFR-A-10-5	0.6	1.08	36.4	30.1	0.0	20.4	28.2	0.26 (0.89)
HTSBFR-A-10-10	0.9	1.61	47.4	36.9	0.7	18.6	27.8	0.28 (0.96)
HTSBFR-A-10-15	0.9	1.70	49.3	37.6	0.7	18.6	27.7	0.30 (1.02)
HTSBFR-A-10-20	0.5	1.67	48.1	36.4	0.1	18.9	27.6	0.32 (1.09)
HTSBFR-B-5-10	0.2	1.34	56.2	47.2	0.0	24.2	27.5	0.32 (1.09)
HTSBFR-B-5-15	0.4	1.47	60.6	49.5	0.2	24.4	27.5	0.33 (1.12)
HTSBFR-B-5-20	0.3	1.49	61.7	49.8	0.2	24.6	27.4	0.34 (1.16)
HTSBFR-B-10-5	0.3	0.58	31.2	25.5	0.0	24.8	27.7	0.30 (1.02)
HTSBFR-B-10-10	0.6	1.15	41.7	35.1	0.0	21.7	27.8	0.28 (0.96)
HTSBFR-B-10-15	0.6	1.29	44.6	36.1	0.0	21.8	27.6	0.30 (1.02)
HTSBFR-B-10-20	0.6	1.34	45.4	36.1	0.0	21.7	27.5	0.31 (1.06)

Table 5. Time Constants at Start-up and at Shutdown for the Subcases of Case HTSBFS

Code	Start-up Two-Time-Constant Model				Start-up One-Time-Constant Model		Shutdown	
	t_s, s	B	τ_1, s	τ_2, s	t_s, s	τ_1, s	τ_3, s	$\dot{Q}_R$, kW (kBtu/h)
HTSBFS-A-5-10	15.2	2.47	46.3	33.4	15.7	11.1	19.2	0 (0)
HTSBFS-A-5-15	15.2	2.47	46.3	33.4	15.7	11.1	19.3	0 (0)
HTSBFS-A-5-20	15.2	2.46	46.9	33.8	15.7	11.4	19.3	0 (0)
HTSBFS-A-10-5	15.2	2.48	42.0	31.2	15.7	9.8	19.0	0 (0)
HTSBFS-A-10-10	15.3	2.75	44.2	31.4	15.8	9.3	19.2	0 (0)
HTSBFS-A-10-15	15.3	2.86	45.2	31.3	15.8	9.2	19.2	0 (0)
HTSBFS-A-10-20	15.2	2.86	45.0	31.2	15.8	9.2	19.3	0 (0)
HTSBFS-B-5-10	15.2	2.24	43.1	32.4	15.6	11.4	19.2	0 (0)
HTSBFS-B-5-15	15.2	2.27	43.8	32.6	15.6	11.5	19.2	0 (0)
HTSBFS-B-5-20	15.2	2.28	44.2	32.7	15.6	11.6	19.3	0 (0)
HTSBFS-B-10-5	15.1	2.07	40.2	31.8	15.5	11.2	19.0	0 (0)
HTSBFS-B-10-10	15.2	2.32	41.7	31.5	15.6	10.4	19.2	0 (0)
HTSBFS-B-10-15	15.2	2.44	43.1	31.5	15.6	10.3	19.2	0 (0)
HTSBFS-B-10-20	15.1	2.54	44.2	31.5	15.6	10.3	19.2	0 (0)

Summary for the start-up condition. Generally, the time constant increases with the IWT and decreases if the fan is off at compressor shutdown and if a bleed port is present. With increasing runtime, the time constant decreases in the heating mode, but increases in the cooling mode. With increasing off-cycle time, the time constant increases if the runtime decreases.

Shutdown Time Constant

As shown in Tables 4 to 7, the value of τ_3 in heating mode appears to be relatively independent of the IWT, the runtime, and the off-cycle time. In the HTSBFR case, τ_3 is around 27.6 s and $\dot{Q}_R$ is around 0.31 kW (1.06 kBtu/h); in the HTSBFS case, $\dot{Q}_R = 0$ and τ_3 is around 19.2 s; in the HTABFR case, τ_3 is around 27.4 s and τ_3 is around 0.29 kW (0.99 kBtu/h); finally, in the HTABFS case, $\dot{Q}_R = 0$ and τ_3 is around 19.9 s. Analyzing these values, it appears that HTSBFR = HTABFR, and HTSBFS = HTABFS, both in terms of the time constant τ_3 and fan power in continuous fan mode, signaling that the presence or absence of a bleed port has no impact on the evolution of the residual capacity in the off-cycle.

Still in heating mode, when the fan is remaining on, τ_3 is about 27 s, which is higher than τ_3 in cases when the fan is stopped at compressor shutdown (about 19s). More residual capacity is recovered if the fan is left running at compressor shutdown. Residual capacity recovery in the FS cases follows fan flow decay.

In the cooling mode, as seen in Table 8, fan heat ($\dot{Q}_R$) translates into negative cooling capacity at compressor shutdown. As seen in Table 8, at compressor shutdown for the CLSBFR case, τ_3 increases when IWT increases from 10°C (50°F) to 20°C (68°F) IWT, indicating a proportionally higher residual capacity recovery with lower IWT. The same holds for the CLSBFS case. Furthermore in this latter case, the average τ_3 values are lower than in the CLSBFR case because the only recoverable capacity is that associated with fan delay and inertia.

TRNSYS MODEL

Time constant models can be used to predict the dynamic evolution of the capacities of heat pumps at start-up and at shutdown in real cases, with no need to know the full characteristics of the heat pump. In this section, a simplified dynamic model of a heat pump for inclusion into the simulation program TRNSYS (SEL 2006) is presented. This simplified model (called TYPE 801 in TRNSYS) combines the time constants developed here with the steady-state values (efficiencies, capacities, compressor power uses) found in the manufacturer's performance data. The two-time-constant model is used in this simplified model for the start-up conditions.

Table 6. Time Constants at Start-up and at Shutdown for the Subcases of Case HTABFR

Code	Start-up Two-Time-Constant Model				Start-up One-Time-Constant odel		Shutdown	
	t_s, s	B	τ_1, s	τ_2 s	t_s, s	τ_1, s	τ_3, s	$\dot{Q}_R$, kW (kBtu/h)
HTABFR-A-5-10	1.2	1.53	48.5	38.5	1.0	19.3	27.5	0.29 / 0.99
HTABFR-A-5-15	1.2	1.57	49.0	38.5	1.0	19.3	27.4	0.30 / 1.02
HTABFR-A-5-20	1.2	1.58	49.5	38.8	1.0	19.3	27.3	0.31 / 1.06
HTABFR-A-10-5	1.2	1.59	49.3	39.2	1.0	19.1	28.3	0.21 / 0.72
HTABFR-A-10-10	1.2	1.58	49.0	38.9	1.0	19.3	27.4	0.29 / 0.99
HTABFR-A-10-15	1.1	1.67	51.0	39.2	0.9	19.4	27.2	0.31 / 1.06
HTABFR-A-10-20	1.1	1.79	53.8	40.0	1.0	19.4	27.2	0.31 / 1.06
HTABFR-B-5-10	0.7	1.00	38.9	33.3	0.0	21.8	27.5	0.28 / 0.96
HTABFR-B-5-15	0.7	1.05	39.7	33.6	0.0	21.7	27.3	0.30 / 1.02
HTABFR-B-5-20	0.7	1.10	40.5	33.6	0.0	21.8	27.2	0.31 / 1.06
HTABFR-B-10-5	0.7	1.00	39.2	34.5	0.0	21.9	28.0	0.20 / 0.68
HTABFR-B-10-10	0.6	1.11	41.5	35.3	0.0	22.0	27.4	0.28 / 0.96
HTABFR-B-10-15	0.6	1.28	45.0	36.5	0.0	22.2	27.2	0.30 / 1.02
HTABFR-B-10-20	0.5	1.41	48.1	37.4	0.0	22.3	27.2	0.31 / 1.06

Average Capacities

In this simplified model, the average capacities are used between the preceding time and the current time according to the TRNSYS practice of reporting average values over a given time step, namely between τ_0 and $t(t - t_0 = \Delta t)$.

On-Cycle Average Capacity. With the compressor running, the variation of the capacity over time is given by Equation 5. It can be shown that, for $t_i \geq t_s$:

$$\begin{aligned} I &= \frac{1}{\dot{Q}_{SS}} \int_{t_i}^{t} \dot{Q} dt \\ &= (t - t_i) + \tau_1 \left[e^{-(t-t_s)/\tau_1} - e^{-(t_i - t_s)/\tau_1} \right] \\ &\quad - B\tau_2 \left[e^{-(t-t_s)/\tau_2} - e^{-(t_i - t_s)/\tau_2} \right] \\ &\quad + \frac{B\tau_1\tau_2}{\tau_1 + \tau_2} \left[e^{-(t-t_s)\left(\frac{1}{\tau_1} + \frac{1}{\tau_2}\right)} - e^{-(t_i - t_s)\left(\frac{1}{\tau_1} + \frac{1}{\tau_2}\right)} \right] \end{aligned} \quad (7)$$

If $t \geq t_s$, then $t_i = t_o$ and if $t_0 < t_s$, then $t_i = t_s$ in Equation 7 and the average capacity during the time step is:

$$\dot{Q}_{av} = \frac{\dot{Q}_{SS}}{\Delta t} I \quad (8)$$

Off-Cycle Average Capacity. In the case where the compressor is not in operation, the variation of the capacity is captured by using Equation 6.

The average capacity is:

$$\dot{Q}_{av} = \frac{1}{\Delta t} \int_{t_0}^{t} \dot{Q} dt = \frac{1}{\Delta t} \int_{t_0}^{t} \left(D\dot{Q}_{SS} e^{-t/\tau_3} + \dot{Q}_R \right) dt \quad (9)$$

$$\dot{Q}_{av} = \frac{D\dot{Q}_{SS}\tau_3}{\Delta t} \left(e^{-t_0/\tau_3} - e^{-t/\tau_3} \right) + \dot{Q}_R \quad (10)$$

For more details on the implementation process of the simplified model into TRNSYS, the reader is referred to Ndiaye (2007).

Simplified Model Illustration

Two application examples of the simplified model in TRNSYS are presented. TYPE 801 is submitted to an input signal (a signal value of 1 means that the heat pump is in operation during the time step), and the response in terms of total and sensible capacities is studied. The first example (Figure 6) is for a heating mode. In the second example (Figure 7), the

Table 7. Time Constants at Start-up and at Shutdown for the Subcases of Case HTABFS

Code	Start-up Two-Time-Constant Model				Start-up One-Time-Constant Model		Shutdown	
	t_s, s	B	τ_1 s	τ_2, s	t_s, s	τ_1, s	τ_3, s	$\dot{Q}_R$, kW (kBtu/h)
HTABFS-A-5-10	20.3	2.66	37.3	27.0	20.7	8.2	20.0	0 (0)
HTABFS-A-5-15	20.3	2.68	37.3	27.0	20.7	8.2	20.0	0 (0)
HTABFS-A-5-20	20.3	2.70	37.7	27.0	20.7	8.2	20.0	0 (0)
HTABFS-A-10-5	20.3	2.64	37.3	27.8	20.8	8.0	19.7	0 (0)
HTABFS-A-10-10	20.3	2.71	37.6	27.3	20.7	8.0	19.9	0 (0)
HTABFS-A-10-15	20.3	2.80	38.6	27.3	20.7	8.0	20.0	0 (0)
HTABFS-A-10-20	20.3	2.88	39.5	27.4	20.7	8.0	20.0	0 (0)
HTABFS-B-5-10	20.2	2.19	34.0	26.4	20.6	9.0	19.9	0 (0)
HTABFS-B-5-15	20.2	2.24	34.5	26.4	20.6	9.0	20.0	0 (0)
HTABFS-B-5-20	20.2	2.27	34.7	26.4	20.6	9.0	20.0	0 (0)
HTABFS-B-10-5	20.2	2.18	34.1	26.9	20.6	9.0	19.6	0 (0)
HTABFS-B-10-10	20.2	2.27	35.0	26.8	20.6	8.9	19.9	0 (0)
HTABFS-B-10-15	20.2	2.36	36.0	26.8	20.6	8.9	19.9	0 (0)
HTABFS-B-10-20	20.2	2.46	37.2	27.0	20.6	8.9	20.0	0 (0)

input signal sets a cooling mode. In both cases, the simulation time step is 15 s and the duration of the simulation is 1 h.

As seen in Figure 6, the heat pump heating capacity gradually grows to its steady-state value at start-up, and gradually decays to zero at compressor shutdown. The same behaviour is observed in Figure 7 for both the total and the sensible cooling capacities. TYPE 801 is consequently responding as expected and can be used to accurately predict the performance of geothermal heat pumps in transient operating conditions.

CONCLUSION

Simplified general models for the evolution of a heat pump capacity at start-up and in the shutdown phase are presented. A two-time-constant model and a one-time-constant model are proposed for the start-up phase. For the shutdown phase, a one-time-constant extinction function is suggested. When tested with data from a validated heat pump model, the time constant models performed very well in capturing the evolutions of the capacities at start-up and at shutdown. The correlation coefficients obtained in these tests are all superior to 0.9 for the start-up phase and to 0.99 for the shutdown phase. It was found that for the start-up phase, the two-time-constant model performs better compared to the one-time-constant model.

Time constants are derived for the start-up and shutdown phases for a large range of heat pump operating conditions. For cooling modes, the time constants are determined for sensible as well as for total capacities. The determined time constants can be used to model the dynamic evolution of the capacities of cycling heat pumps at start-up and at shutdown, in real cases, and with no need to know the full characteristics of the heat pump. This approach is successfully used in this paper to build a TRNSYS type.

In consulting the available literature, the major impression is that the time constant used to model the capacity at start-up has a constant value for a given heat pump. The results presented in this paper show that in fact the time constant varies according to the operating conditions, with values ranging from 0.1 to 27 s. More specifically, it was found that the time constant generally (1) decreases when the runtime increases in the heating mode; (2) increases with the runtime in the cooling mode; (3) decreases for cases where the fan is off at compressor shutdown compared to cases where it remains on; (4) increases with the IWT; and (5) decreases for cases where the expansion valve has a bleed port compared to cases where there is no bleed port in the expansion valve.

ACKNOWLEDGMENTS

The National Sciences and Engineering Research Council of Canada (NSERC), the CANMET Energy Technology

Table 8. Time Constants at Start-up and at Shutdown for the Subcases of Case CLSBFR

Code		Start-up Two-Time-Constant Model				Start-up One-Time-Constant Model		Shutdown	
		t_s, s	B	τ_1, s	t_2, s	τ_s s	τ_1 s	τ_3, s	$\dot{Q}_R$, kW (kBtu/h)
CLSBFR-A-5-10	SEN	3.1	1.74	77.5	60.6	3.2	26.9	45.4	–0.39 (–1.33)
	TOT	1.9	1.01	41.3	37.0	1.5	22.0	28.6	–0.31 (–1.06)
CLSBFR-A-5-15	SEN	3.1	1.73	77.5	60.2	3.2	26.9	45.4	–0.37 (–1.26)
	TOT	1.9	1.00	41.0	37.0	1.5	21.9	28.7	–0.32 (–1.09)
CLSBFR-A-5-20	SEN	3.0	1.74	77.5	60.6	3.2	26.8	45.2	–0.36 (–1.23)
	TOT	1.9	1.00	41.2	37.0	1.5	21.9	28.7	–0.33 (–1.12)
CLSBFR-A-10-5	SEN	3.1	1.35	64.9	58.1	3.2	26.9	46.9	–0.48 (–1.64)
	TOT	1.9	.94	39.4	35.7	1.4	22.3	28.2	–0.24 (–0.82)
CLSBFR-A-10-10	SEN	3.1	1.36	65.4	58.5	3.2	27.0	45.7	–0.39 (–1.33)
	TOT	1.9	.94	39.5	35.8	1.4	22.3	28.6	–0.31 –1.06)
CLSBFR-A-10-15	SEN	3.1	1.35	64.9	58.5	3.2	26.9	45.4	–0.37 (–1.26)
	TOT	1.9	.94	39.4	35.8	1.5	22.3	28.8	–0.32 (–1.09)
CLSBFR-A-10-20	SEN	3.1	1.37	65.4	58.5	3.2	26.9	45.2	–0.36 (–1.23)
	TOT	1.9	0.94	39.5	36.1	1.4	22.2	28.8	–0.33 (–1.12)
CLSBFR-B-5-10	SEN	2.9	0.92	36.2	22.9	1.4	26.5	27.0	–0.30 (–1.02)
	TOT	2.5	1.15	31.3	17.2	0.6	23.5	20.9	–0.27 (–0.92)
CLSBFR-B-5-15	SEN	2.9	0.92	36.2	22.8	1.4	26.6	27.0	–0.30 (–1.02)
	TOT	2.5	1.15	31.3	17.1	0.6	23.6	21.0	–0.28 (–0.96)
CLSBFR-B-5-20	SEN	2.9	0.92	36.2	22.8	1.4	26.6	27.1	–0.31 (–1.06)
	TOT	2.5	1.15	31.3	17.1	0.6	23.6	21.0	–0.29 (–0.99)
CLSBFR-B-10-5	SEN	1.9	0.90	36.9	26.1	0.1	26.6	28.6	–0.29 (–0.99)
	TOT	2.1	1.21	32.2	20.2	0.3	22.0	20.7	–0.23 (–0.78)
CLSBFR-B-10-10	SEN	3.1	0.87	35.7	23.2	1.6	27.0	27.3	–0.22 (–0.75)
	TOT	2.6	1.09	31.0	17.5	0.8	23.8	20.0	–0.18 (–0.61)
CLSBFR-B-10-15	SEN	3.1	0.87	35.6	23.0	1.6	27.1	27.5	–0.24 (–0.82)
	TOT	2.6	1.09	30.9	17.3	0.8	23.9	20.1	–0.20 (–0.68)
CLSBFR-B-10-20	SEN	3.1	0.87	35.6	23.0	1.6	27.1	27.8	–0.25 (–0.85)
	TOT	2.6	1.08	30.9	17.3	0.8	23.9	20.3	–0.22 (–0.75)

Centre of Natural Resources Canada, and the Quebec-based heat pump manufacturer ThermoPlus provided financial and logistic supports.

NOMENCLATURE

A = regression parameter
AB = expansion valve with bleed port
B = regression parameter
D = regression parameter
CL = cooling
FR = fan running at compressor shutdown
FS = fan stopped at compressor shutdown
HT = heating
IWT = inlet water temperature, °C (°F)

Table 9. Time Constant at Start-up and at Shutdown for the Subcases of Case CLSBFS

Code		Start-up Two-Time-Constant Model				Start-up One-Time-Constant Model		Shutdown	
		t_s, s	B	τ_1, s	τ_2, s	t_s, s	τ_1, s	τ_3, s	$\dot{Q}_R$, kW (kBtu/h)
CLSBFS-A-5-10	SEN	15.2	2.24	38.9	21.9	13.7	15.5	26.0	0 (0)
	TOT	14.6	3.33	32.2	15.2	13.5	9.5	16.9	0 (0)
CLSBFS-A-5-15	SEN	15.2	2.23	38.8	21.9	13.7	15.6	26.0	0 (0)
	TOT	14.6	3.32	32.2	15.1	13.5	9.5	17.0	0 (0)
CLSBFS-A-5-20	SEN	15.2	2.24	38.9	21.9	13.7	15.5	26.0	0 (0)
	TOT	14.6	3.32	32.2	15.2	13.5	9.4	17.1	0 (0)
CLSBFS-A-10-5	SEN	15.2	2.11	36.6	21.2	13.0	16.9	25.9	0 (0)
	TOT	14.7	3.29	31.5	14.8	12.2	11.6	16.5	0 (0)
CLSBFS-A-10-10	SEN	15.2	2.12	36.8	21.3	13.1	16.9	26.0	0 (0)
	TOT	14.7	3.28	31.5	14.8	12.4	11.4	16.9	0 (0)
CLSBFS-A-10-15	SEN	15.2	2.14	37.2	21.8	13.4	16.3	26.0	0 (0)
	TOT	14.7	3.30	32.0	15.3	13.1	10.3	17.1	0 (0)
CLSBFS-A-10-20	SEN	15.2	2.15	37.4	21.9	13.4	16.3	26.0	0 (0)
	TOT	14.7	3.29	31.9	15.3	13.2	10.1	17.2	0 (0)
CLSBFS-B-5-10	SEN	14.8	0.55	23.5	14.7	13.2	21.1	20.7	0 (0)
	TOT	14.7	2.29	20.6	7.4	7.9	21.4	13.7	0 (0)
CLSBFS-B-5-15	SEN	14.8	0.56	23.6	14.8	13.2	21.1	20.8	0 (0)
	TOT	14.7	2.30	20.6	7.4	7.8	21.4	13.9	0 (0)
CLSBFS-B-5-20	SEN	14.8	0.56	23.6	14.8	13.2	21.2	20.9	0 (0)
	TOT	14.7	2.30	20.6	7.4	7.8	21.5	13.9	0 (0)
CLSBFS-B-10-5	SEN	15.0	6.23	19.0	5.8	15.0	2.2	21.7	0 (0)
	TOT	15.0	12.03	15.1	3.3	15.0	0.1	14.0	0 (0)
CLSBFS-B-10-10	SEN	14.6	0.58	22.3	14.2	15.0	17.9	23.7	0 (0)
	TOT	14.7	2.34	19.5	7.1	15.0	13.2	15.9	0 (0)
CLSBFS-B-10-15	SEN	14.6	0.57	22.2	14.0	15.0	18.0	23.7	0 (0)
	TOT	14.7	2.37	19.4	6.9	15.0	13.4	16.0	0 (0)
CLSBFS-B-10-20	SEN	15.0	6.32	19.2	5.8	15.0	2.2	22.0	0 (0)
	TOT	15.0	12.27	15.2	3.3	15.0	0.1	14.6	0 (0)

$\dot{Q}$ = capacity, W (Btu/h)
R^2 = goodness-of-fit of regression
SB = expansion valve without bleed port
t = time, s

Greek Letters

Δ = differential
τ = time constant, s

Subscripts

av = average
i = time index
0 = initial
R = residual

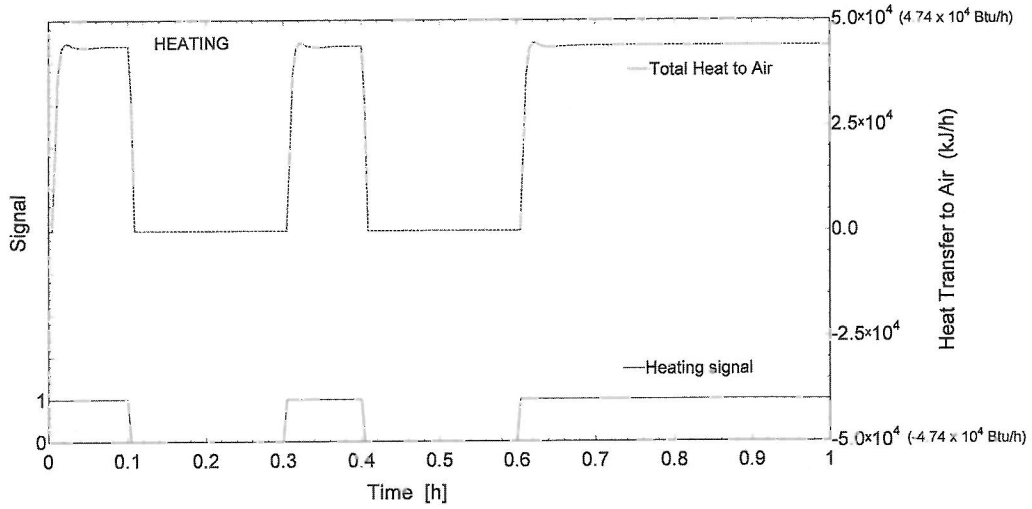

Figure 6 *TRNSYS screen capture showing the response of TYPE 801 to a heating input signal.*

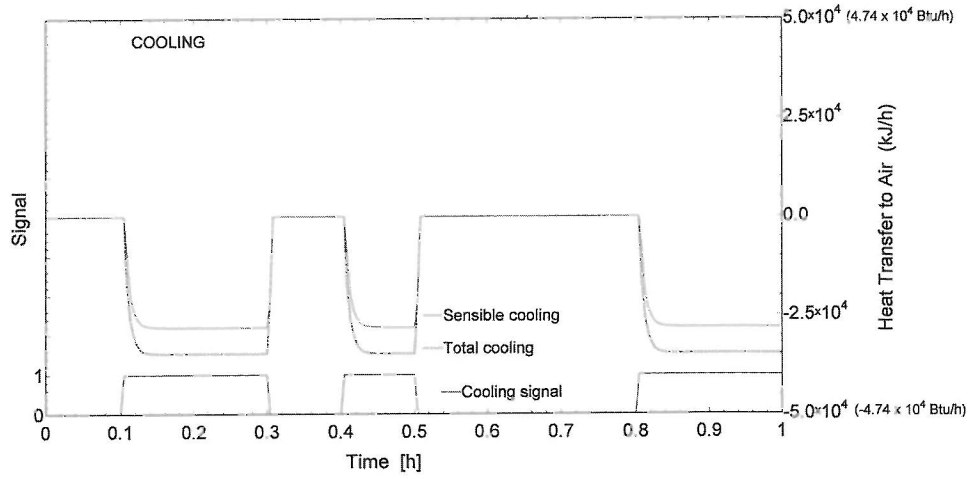

Figure 7 *TRNSYS screen capture showing the response of TYPE 801 to a cooling input signal.*

S = capacity growth start time
SS = steady-state

REFERENCES

CAN/CSA. 2001. CAN/CSA-C13256-1-01, Water-Source heat Pumps—Testing and Rating Performance—Part 1: Water-toWater and Brine-to-Air. CSA.

Goldschmidt, V.W., G.H. Hart, and R.C. Reiner. 1980. A note on the transient performance and degradation coefficient of a field tested heat pump – cooling and heating mode. *ASHRAE Transactions* 86(2):368–75.

Katipamula, S., and D.L. O'Neal. 1991. Performance degradation during on-off cycling of single-speed heat pumps operating in the cooling mode: Experimental results. *ASHRAE Transactions* 97(2):331–39.

Mulroy, W.J., and D.A. Didion. 1985. Refrigerant migration in a split-unit air conditioner. *ASHRAE Transactions* 91(1A):193–206.

Murphy, W.E., and V.W. Goldschmidt. 1979. The degradation coefficient of a field-tested self-contained 3-ton air conditioner. *ASHRAE Transactions* 85(2):396–405.

Ndiaye, D. 2007. Étude numérique et expérimentale de la performance en régime transitoire de pompes à chaleur eau – air en cyclage. *PhD Dissertation*, Département de génie mécanique, École Polytechnique de Montréal, Université de Montréal, Montreal, QC, Canada.

Ndiaye, D., and M. Bernier. 2009. Modelling the bleed port of a thermostatic expansion valve. *International Journal of Refrigeration* 32(5)826–36.

Ndiaye, D., and M. Bernier. 2010a. Dynamic model of a hermetic reciprocating compressor in on-off cycling operation. *Applied Thermal Engineering* 30:792–99.

Ndiaye, D., and M. Bernier. 2010b. Transient modeling of refrigerant-to-air fin-and-tube heat exchangers. *HVAC&R Research* 16(3):355–81.

Ndiaye, D., and M. Bernier. 2012a. Transient model of a geothermal heat pump in cycling conditions – part A: the model. *International Journal of Refrigeration* 35(8)2110–23.

Ndiaye, D., and M. Bernier. 2012b. Transient model of a geothermal heat pump in cycling conditions – part A: experimental validation and results. *International Journal of Refrigeration* 35(8)2124-37.

O'Neal, D.L., and S. Katipamula. 1991. Performance degradation during on-off cycling of single-speed air conditioners and heat pumps: model development and analysis. *ASHRAE Transactions* 97(2):316–23.

Patankar, S.V. 1980. *Numerical Heat Transfer and Fluid Flow.* Washington, New York: Hemisphere Pub. Corp. McGraw-Hill, 197 p.

SEL. 2006. *TRNSYS.* Madison, WI: University of Wisconsin.

Votsis, P.P., S.A. Tassou, D.R. Wilson, and C.J. Marquand. 1992. Dynamic characteristics of an air-to-water heat pump system. *International Journal of Refrigeration* 15(2):89–94.